Experimental Investigation of Forces Produced by Misaligned Steel Rollers

Timothy Krantz*, Christopher DellaCorte* and Michael Dube**

Abstract

The International Space Station Solar Alpha Rotary Joint (SARJ) uses a roller-based mechanism for positioning of the solar arrays. The forces and moments that develop at the roller interfaces are influenced by the design including the kinematic constraints and the lubrication condition. To help understand the SARJ operation, a set of dedicated experiments were completed using roller pairs. Of primary interest was to measure the axial force directed along the axis of rotation of the roller as a function of shaft misalignment. The conditions studied included dry and clean surfaces; one surface plated by a gold film, and greased surfaces. For the case of a bare 440C roller against a nitrided 15-5 roller without lubrication, the axial force can be as great as 0.4 times the normal load for a shaft angle of 0.5 degree. Such a magnitude of force on a roller in the SARJ mechanism would cause roller tipping and contact pressures much greater than anticipated by the designers. For the case of a bare 440C roller against a nitrided 15-5 roller with grease lubrication, the axial force does not exceed about 0.15 times the normal load even for the largest misalignment angles tested. Gold films provided good lubrication for the short duration testing reported herein. Grease lubrication limited the magnitude of the axial force to even smaller magnitudes than was achieved with the gold films. The experiments demonstrate the critical role of good lubrication for the SARJ mechanism.

Introduction

The International Space Station makes use of a roller-based mechanism for positioning of the solar arrays. The fundamental concept of the roller-based mechanism of the Solar Alpha Rotary Joint is described by Loewenthal and Schuller [1]. A careful study of the SARJ system reveals an interesting and significant interplay of forces at the interface where the rollers of the rotary joint mechanism touches the large rotating ring. It is well established in the literature that forces and moments can develop at the interacting surfaces in rolling and sliding contact [2,3]. The forces and moments that develop are influenced by the details of the design including the kinematic constraints. Proper understanding of the influence of roller misalignment has proven to be important in the development of a roller mechanism used for positioning of a radio astronomy antenna [4,5,6]. The influence of roller misalignment is likewise important for the operation of the SARJ mechanism.

The roller and ring of the SARJ mechanism and the meaning of the term “shaft misalignment” is depicted in schematic form in Figure 1. The SARJ rollers are constrained to rotate about shaft axes that nominally intersect the rotational axis of the ring (Figure 1 [a-b]). Any deviation from perfect alignment of a roller axis and ring axis (Figure 1[c]) will give rise to a force at the contact interface in the direction of the roller shaft axis (termed herein the axial force). The magnitude of the axial force will depend on the magnitude of misalignment, the normal load on the roller, the stiffness of the system, the torque transmitted by the roller, and frictional condition of the contacting surfaces. The SARJ mechanism was built to high precision, and the installed roller shaft angle (misalignment) was within a fraction of a degree to perfect alignment. As will be evident from this study, misalignments of even such small magnitude can produce significant forces that influence the performance of the mechanism.

* NASA Glenn Research Center, Cleveland, OH
** NASA Goddard Space Flight Center, Greenbelt, MD

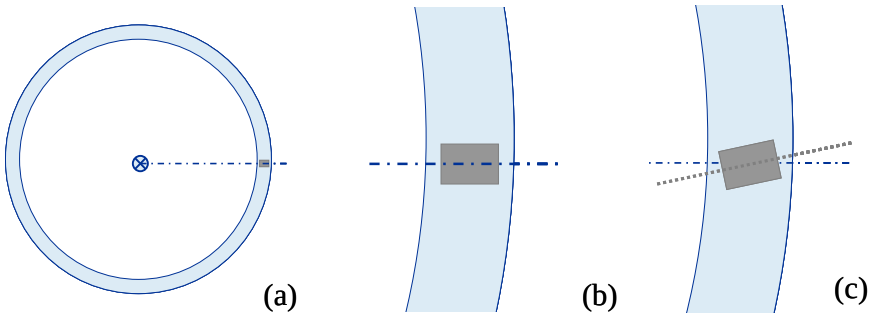

Figure 1 - SARJ ring and roller schematic, top view. (a) Overall view, roller axis aligned with ring axis; (b) close-up view near roller, aligned axis; (c) close-up view near roller, roller axis misaligned (misalignment magnitude greatly exaggerated).

The axial force that develops in response to the misalignment of the axes can have a significant influence on the operating conditions of the SARJ hardware. The axial force and the associated moment that arise from misaligned axes are carried by a pair of tapered roller bearings via the roller shaft to the roller housing. The axial force interacts through a pivot point in the roller housing (Figure 2). In the absence of misalignment, the pivot point allows for uniform contact of the nominally flat roller profile contacting the nominally flat raceway surface. But for the case of misaligned axes, the axial force acts via the pivot point and produces a non-uniform contact pressure across the roller profile. Note from Figure 2 the moments created by the normal load and axial force acting via the pivot point must be balanced for static equilibrium. Thereby, the axial force acts to shift the position of the resultant normal load along the face of the ring and roller contact. The axial force arising from misaligned axes can, if of sufficient magnitude, cause tipping of the roller. Also note that the axial force acting on a roller is carried to the roller shaft via a pair of lightly-preloaded tapered roller bearings. The magnitude of the axial force influences the drag torque of the bearings and thereby influences the torque required to rotate the mechanism.

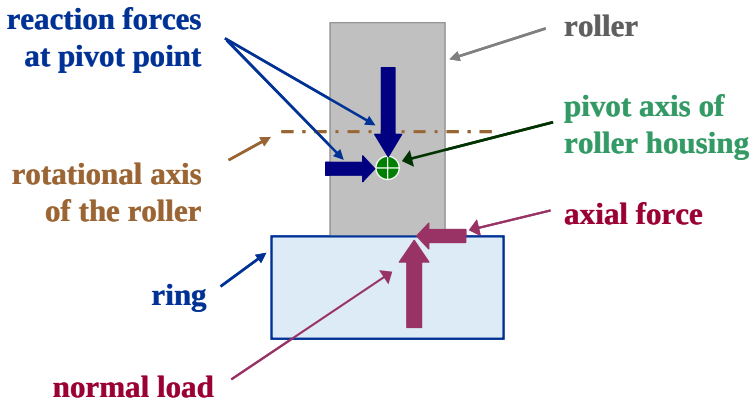

Figure 2 - Schematic of the SARJ roller and ring in contact, front view. Illustrated are the forces imposed by the ring on the roller and the reaction forces at the pivot point in the roller housing.

To help understand the SARJ mechanism operation, a set of dedicated experiments were completed using roller pairs. The purpose of the experiments was to quantify the relationship of the misalignment of roller axes to the resulting forces that develop. The relationship of shaft axis misalignment magnitude to axial force magnitude was determined for the material combination used in the SARJ mechanism for a variety of surface and environment conditions as can influence the friction and, thereby, the behavior of the mechanism.

Apparatus, Specimens, and Procedures

Test Apparatus for Roller Pairs

Testing was done using the NASA Glenn Research Center Vacuum Roller Rig (Figure 3). The rig allows for application and measurement of a load pressing the rollers together while having a purposely misaligned and adjustable shaft angle. The rig is depicted in schematic form in Figure 4. A drive motor provides motion to the driving roller. A magnetic-particle brake attached to the output shaft imposes torque on the driven roller. The rig can be operated with the brake not energized. For such a condition the torque transmitted through the roller pair is only the drag torque of the output shaft (drag of the seals and support bearings). The normal load pressing the rollers together is provided by an air cylinder. The cylinder acts through a gimbal point to rotate the plate that mounts the driving shaft and drive motor. The rotation of the drive motor plate displaces the driving roller toward the driven roller shaft. The pressure to the cylinder, and thereby the load between the contacting rollers, is adjusted by a hand-operated valve (open-loop control). Testing can be done in vacuum or ambient air. Vacuum is provided by a diffusion pump with a liquid nitrogen cold trap. The diffusion pump is assisted by a mechanical vacuum pump. Figure 5 provides a simplified schematic labeled with some of the nomenclature used herein.

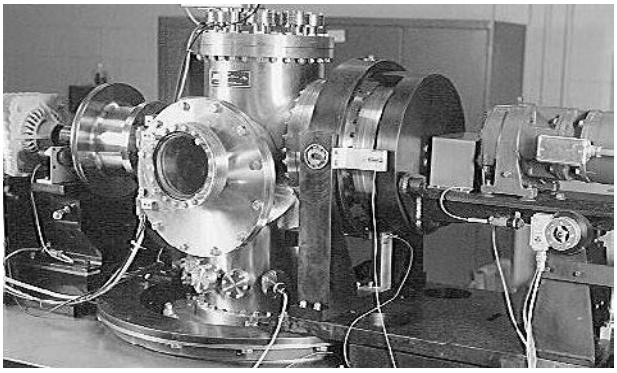

Figure 3 – Vacuum roller rig.

A set of sensors on the test apparatus monitors the test conditions. The outputs of the analog sensors were digitized and stored via a data collection unit at a rate of 0.66 Hz. Each of the sensors and the methods of calibration will be described in turn.

The misalignment of the driving roller shaft and driven roller shaft is depicted in an exaggerated manner in Figure 4(b). The misalignment is measured via a linear variable differential transformer (LVDT). The transducer housing is attached to the bedplate, and the translating, spring-loaded transducer tip contacts against a mechanical stop on the turntable. The mechanical stop is mounted at a known radial distance and tangential orientation from the center of the turntable. Calibrated gage blocks were used to displace the transducer by known amounts, and using the rig geometry the equivalent angular rotation of the turntable was calculated. The preceding steps established the relationship of change in transducer output to the change in relative shaft angle. To establish the aligned condition, a special tooling block was machined to locate the roller-mounting surfaces of the two shafts as parallel. With the shafts aligned by the tooling block, the transducer circuit balance was adjusted to provide an output of zero. The precision of this method for aligning the shafts was limited by the dimensions of the roller mounting surfaces used as the reference planes. From the test rig drawing tolerances and geometry, the alignment procedure using the tooling block to define the zero-degree position has an accuracy of no better than 0.11 degree.

The torque on the output shaft is monitored by a strain-gage type torquemeter of 22 N-m (200 in-lb) torque capacity. Calibration was done in place using deadweights acting on a torque arm of known length.

The load that presses the rollers together is termed herein the “normal load” (Figure 5). The normal load is applied via an air-pressure actuated piston. The air piston acts through a load cell against the drive motor plate that is gimbal-mounted relative to the test chamber (Figure 4(a)). In this way the air cylinder moves the roller on the input shaft in an arc motion toward the test roller. Once the rollers are in contact, additional force commanded from the air cylinder increases the normal load between the test rollers. The force sensed by the load cell located between the gimbaled motor plate and the air piston is a linear combination of two sources, the unbalanced mass relative to the gimbal point and the normal load on the test roller.

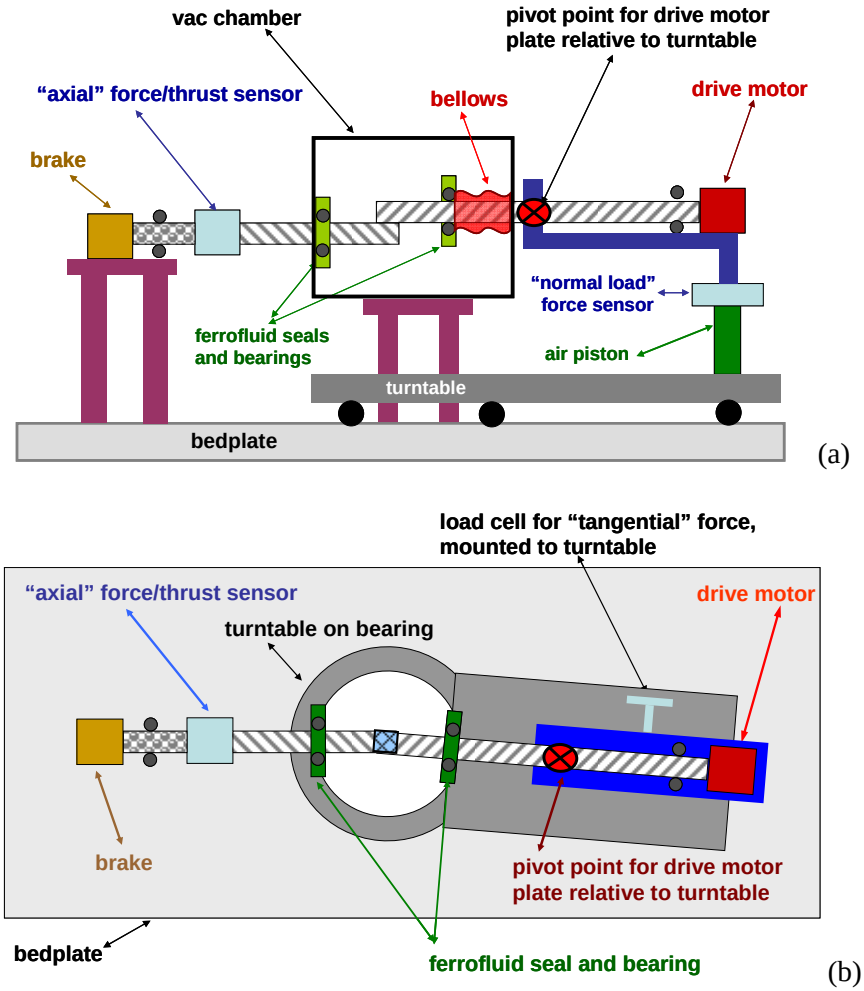

Figure 4 – Schematic views of the vacuum roller rig. (a) Schematic, side view. (b) Schematic, overhead view with shaft misalignment depicted and exaggerated.

The following calibration procedure was used so that the two sources influencing the load cell output during testing could be separated. First the load cell was removed from the rig, calibrated using deadweights, and reinstalled on the test apparatus. Next, a LVDT was used to monitor the displacement of the motor plate. With no test roller installed on the output shaft, the air piston was used to move the motor plate through the full range of motion while recording the output of the calibrated load cell. In this manner the force as sensed at the load cell due to the unbalanced mass of the gimbaled motor plate was determined as a function of the motor plate position. Next, the end of the input shaft where the test roller is mounted was attached by a highly-rigid link to the apparatus frame. The rigid link included a calibrated reference load cell in the load path. The rigid link was carefully positioned to be oriented in the position and direction of the normal load created between the contacting test rollers. By increasing the pressure

on the air-piston actuator, load was created on the rigid link and measured on the reference load cell. This procedure established the relationship of the normal load on the test roller acting through the gimbal point and resulting in a force imparted on the load cell located at the air piston. During testing both the motor table position and load cell force was recorded. From the table position data and calibration data, the force attributed to the unbalanced mass on the gimbaled motor plate could be subtracted from the force value recorded by the load cell. The value remaining from the load cell (after the subtraction operation) is due to the normal force between the test rollers, and via the calibration curve the load on the test roller is determined.

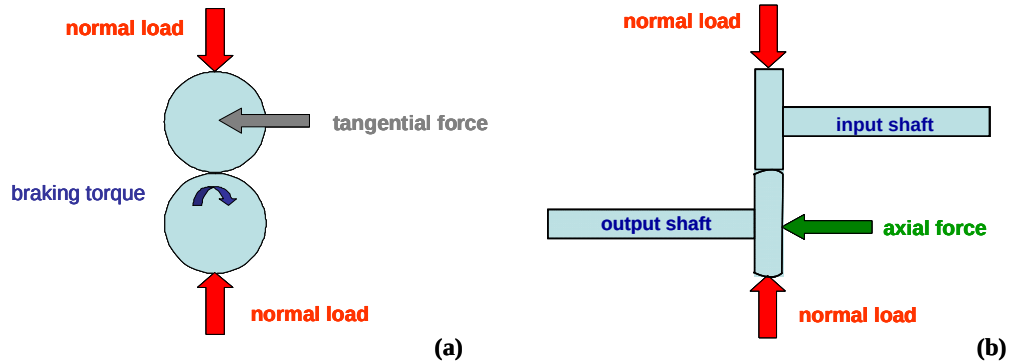

Figure 5 – Simplified schematic view including some of the important sensed data. (a) Schematic, front view. (b) Schematic, side view.

When rollers operate in a misaligned condition a force will develop in the direction of the shaft axis [2,3,5,6]. In such a condition points on the two rollers in intimate contact and within a “stick” zone of the contact patch are constrained to move in unison. If the points were not in contact the kinematic constraints would provide a slightly different path of motion. The difference in the actual path of motion and that defined by the motion if the points were not in contact gives rise to surface strains and a resultant axial force. A sensor to measure this force is labeled as the “axial force” sensor in Figure 4. The axial force sensor is co-located on the output shaft with the torquemeter sensor. The configuration of the rig did not allow for direct deadweight calibration in place. To calibrate the sensor in place, the following procedure was used. First, a load cell was calibrated via deadweights and then was placed on the free end of the output shaft to act as a reference load cell. A threaded jackscrew acted against the reference load cell and a hard stop in the vacuum chamber. Adjusting the jackscrew length allowed for changing the force imparted on both the reference load cell and, the rig’s axial load cell and to the machine frame. In this manner the same force was applied to both load cells, and the reference cell output used to calibrate the axial load cell sensor in place.

The preceding two paragraphs describe the sensors (and sensor calibrations) to determine two mutually perpendicular forces acting on the driven test roller. A force also acts along a third axis. This is the force directed tangential to the roller diameter and is termed here as the “tangential” force. The tangential force on the input shaft roller acts through a gimbal point (Figure 4(b)). The rotational motion about the gimbal point is restrained by a mechanical link to the turntable structure. There is a load cell load in the load path from said mechanical link to the turntable structure. This sensor was calibrated in place by using a pulley-cable system and dead weights to relate the tangential force applied at the test roller position to the sensor output. During testing, this sensor is also affected by spin moments (Ref. (2)) that can develop in roller contacts. The data from the tangential force sensor was recorded for possible future use, but such data were not of immediate interest and are not reported herein.

Shaft speeds and total number of shaft revolutions were measured using encoders on each shaft. The encoder pulses were counted and recorded via a digital pulse counter. The encoder pulses were also monitored by a frequency converter to provide a convenient shaft speed display to the test operator. The encoders provide 6,000 pulses for each shaft revolution.

The pressure in the chamber was monitored by an ionization gauge at the top of the main test chamber. The typical pressure in the testing chamber during vacuum testing was $5x10^{-6}$ Torr. Vacuum is provided by a diffusion pump with a liquid nitrogen cold trap. The diffusion pump is assisted by a mechanical vacuum pump. The diffusion pump and cold trap arrangement prevents oil vapors from the mechanical vacuum pump to enter the test chamber so as to maintain the desired tribological test condition.

Test Specimens

The test specimens used for this research had a nominal geometry of 35.6-mm (1.4-inch) outer diameter and a 12.7-mm (0.5-inch) width. The roller on the drive motor (input) shaft was made from 15-5 alloy (matching the SARJ raceway material). The roller on the brake (output) shaft was 440C alloy, matching the SARJ roller material. A set of nitrided 15-5 rollers were manufactured to match the processing parameters of the SARJ ring. An additional set of 15-5 rollers without nitriding were manufactured for research purposes. In the remainder of this document we use the term “un-nitrided” to refer to a 15-5 roller that does not have the nitride surface layer. The profile across the roller width for the 15-5 rollers was nominally flat. The mating 440C rollers used for this project had a crown radius profile across the roller width. For the test apparatus used, at least one of the two rollers must be crowned to have a controlled contact condition. The nominal crown radius of the 440C test rollers for this project was approximately 42 mm (1.65 inch). The 440C rollers had a measured surface hardness via a Rockwell tester of typically 56 HRC. The SARJ mechanism makes use of gold-plated rollers. A subset of the 440C rollers were provided with gold plating. All of the gold-plated test rollers were done in a single batch process. The plating vendor reported the applied gold layer thickness as 2300 angstroms.

A photograph of a pair of rollers installed and undergoing test is provided in Figure 6. The upper roller is a 15-5 roller with a nominally flat profile. The bottom roller is the 440C roller having a crown radius. The localized contact provided by the crowned roller is evident in Figure 6.

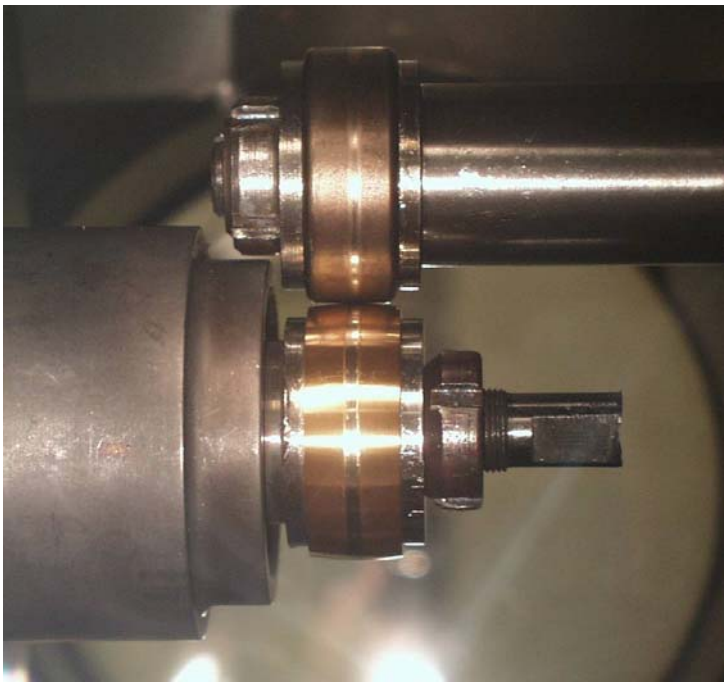

Figure 6 – View of tested rollers in the test apparatus showing localization of the roller contact and crowned profile of the lower roller.

To document the surface condition of the new rollers, rollers were inspected via a stylus profilometer using a diamond-tipped stylus. The data were processed to assess the roughness features. The roughness of a 440C roller was typically 0.14 micrometer roughness-average. The roughness of a nitrided 15-5 roller was typically 0.62 micrometer roughness-average. Plots of the roughness profile for a typical 440C and nitrided 15-5 roller are provided in Figures 7-8 (note the differing automatic scaling used in these two figures).

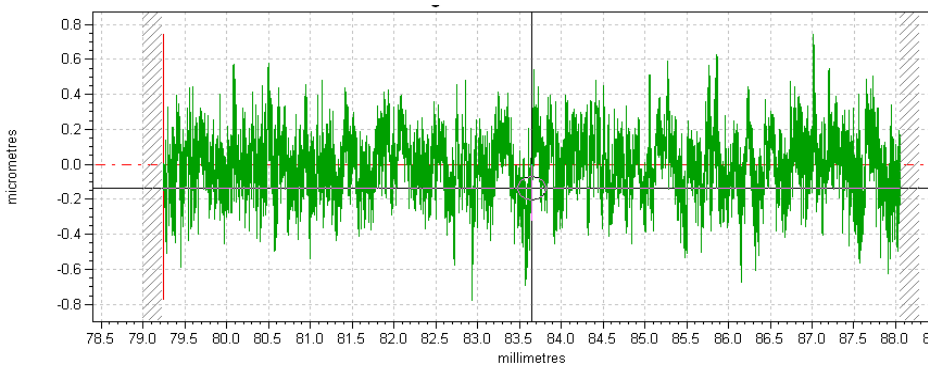

Figure 7 - Typical roughness of a 440C roller.

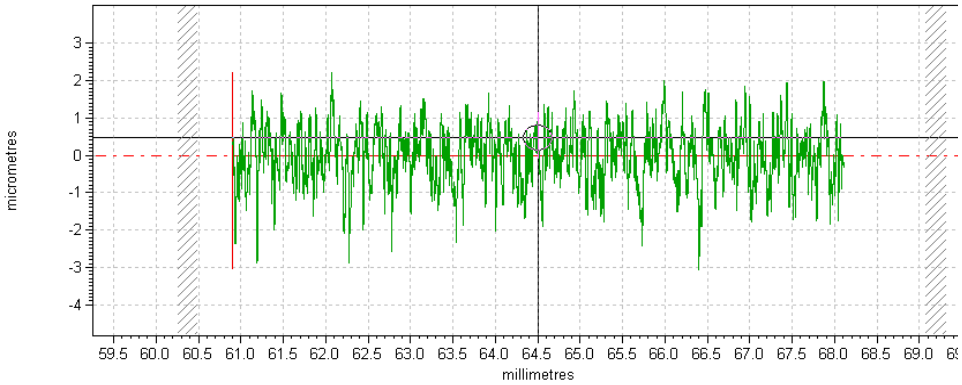

Figure 8 - Typical roughness of a nitrided roller.

Procedure to Install Test Rollers

Test specimens were cleaned and installed using careful procedures to provide a clean test surface. The 15-5 test rollers were cleaned just prior to installation into the rig using de-ionized water and 0.05 micron alumina powder. After appropriate hand scrubbing, the cleaning powder was rinsed with deionized water making sure that the entire roller surface wetted uniformly to confirm complete cleaning of surface oils. The water was removed from the roller using dried pressurized nitrogen. Bare (without gold-plating) 440C specimens were cleaned in the same manner as the 15-5 specimens. The 440C test rollers with gold-plating were vacuum-sealed in plastic bags by the plating vendor, and so cleaning with alumina powder was not needed. The bags remained closed until ready for installation. Test rollers and mounting hardware were handled only with gloved hands and clean tools to complete installation into the test apparatus.

Procedure for Testing Rollers

The first step for testing after installation of the test rollers was to immediately isolate the testing chamber and provide a vacuum, using the mechanical roughing pump, to approximately 50×10^{-3} Torr chamber pressure. This isolation step was done even if test scheduling required some delay between the time of installation of rollers and the time for testing to minimize exposure of the cleaned surfaces to any contaminants that might be present in the atmosphere. Just prior to testing the diffusion pump was energized and the pressure in the testing chamber established to approximately 5×10^{-6} Torr.

Some tests were done to investigate the influence of grease lubrication of the performance of the contacting rollers. For these tests the roller surfaces were lubricated using a space-qualified grease. The base oil of the grease is a stable perfluorinated polyether. The gelling agent is a tetrafluoroethylene telomer. The grease contains molybdenum disulfide. The grease was applied using a syringe. The difference in the mass of the syringe before and after applying the grease was 0.34 gram. The grease was distributed on the rollers by positioning the rollers with only a small gap between them and the shafts were rotated. As the grease became distributed by the shaft rotation the gap between the rollers was slowly reduced in increments. This action proved effective to distribute the grease about the roller circumference, and by visual inspection the distribution of the grease about the roller circumference appeared uniform.

Once rollers were installed and the chamber pressure test condition was established, the next step of the test procedure was to “run-in” the roller surfaces. In general contacting surfaces will quickly “run-in” via wear and deformation of asperity features. The test rig shaft misalignment angle was set to 1.5 degrees and the rollers were brought into contact with approximately 667 N (150 lb) normal force between the rollers. The test rig was operated for at least 1000 shaft revolutions to run-in the test surfaces.

The third step of the test procedure was to smoothly and continuously change the misalignment angle while recording data to investigate the traction capability of the contact. This step was done to establish the relationship of the misalignment angle to the developed axial force. The misalignment angle was changed by hand-turning of a threaded rod to rotate the turntable relative to the rig bedplate. The misalignment angle was swept from a position of approximately 1.5 degrees to a position of -1.5 degrees, and after a short pause the direction reversed and the angle adjusted again in a smooth fashion back to the starting angle of 1.5 degrees. The angle adjustment occurred over a time of approximately three minutes. During these sweeps of the misalignment angle the magnetic-particle brake on the output shaft was not energized, and the recorded torque on the output shaft was in the range 0.8~1.2 N-m (7~11 in-lb). The procedure to adjust the misalignment angle was repeated for 3 values of the normal load, approximately 445, 667, and 890 N (100, 150, and 200 lb).

The preceding paragraphs described the procedure to investigate the behavior of the contact with small torque transmitted buy the roller pair. Next, a test was completed to assess the relationship of axial force as a function of the torque transmitted by the rollers for a condition of shaft misalignment of 1.5 degrees. The rollers were the same roller pair as described in the preceding paragraph. The rig was operated at a speed of approximately 15 rpm. The test was done in vacuum of $5x10^{-6}$ Torr. The normal load between the rollers was 436 N (98 lb). With the test operating, the braking torque on the output shaft was adjusted until the output shaft was at a near stall condition because of the high braking torque. The data was processed to determine the measured axial force as a function of the torque transmitted by the roller pair.

Test Results

Axial Force as a Function of Shaft Misalignment Angle

Data were recorded and processed to determine the axial force created in the direction of the rotational axis of the output shaft as a function of the operating condition. The array of testing that was performed is documented in Table I. Each of the test conditions of Table I were repeated for 3 levels of applied normal load, the targeted loads being 445, 667, and 890 N (100, 150, and 200 lb). A Hertz contact analysis was completed for each of the three targeted load using the calculation method of Hamrock and Brewe [7]. The maximum calculated contact pressures for these loads are 1.55, 1.79, and 1.97 GPa (225,000, 260,000, and 285,000 psi) respectively. The measured loads (as opposed to the targeted test loads) were used for the processing and reporting of data and results.

The axial force that developed in the contact was measured and plotted as a function of the misalignment angle. Figure 9 is a plot of data for the case of un-nitrided 15-5 roller with a 440C roller in a vacuum environment for three levels of normal load. The data has been plotted as a ratio of the measured axial force to the measured normal load as a function of shaft misalignment angle. The data shows that, for

practical engineering purposes of this investigation, the functional relationship of the axial force/normal load ratio to shaft misalignment angle is not strongly influenced by changes in the normal load. To simplify the plotting and discussion of data, the results for the three levels of normal load were treated as a single dataset for the remainder of this report.

Table I – Test Conditions

Roller on input shaft	Roller on output shaft	Grease lubrication?	Chamber condition
un-nitrided 15-5	440C – no plating	no	vacuum
un-nitrided 15-5	440C – no plating	yes	vacuum
nitrided 15-5	440C – no plating	no	vacuum
nitrided 15-5	440C – gold plating	no	vacuum
nitrided 15-5	440C – no plating	yes	vacuum
nitrided 15-5	440C – no plating	no	ambient air

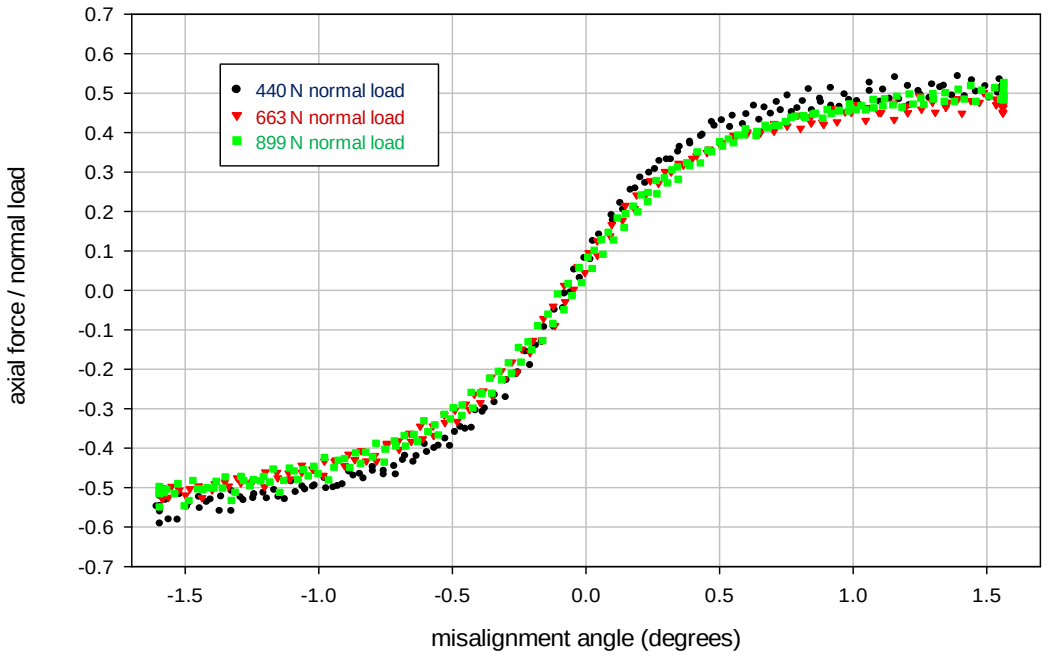

Figure 9 – Ratio of axial load to normal load for three levels of normal load. Test conditions were nitrided 15-5 roller vs. bare 440C (no plating) roller, no grease, in vacuum.

The results of testing at three levels of normal load for the case of a 440C roller mated with a nitrided 15-5 roller and operated in a vacuum are provided in Figure 10. For the case of a bare (un-plated) 440C roller against a nitrided 15-5 roller and without lubrication, the axial force can be as great as 0.4 times the normal load for a shaft angle of 0.5 degree. Experiments and analysis done by others have shown that such a magnitude of force on a SARJ roller would cause roller tipping and contact pressures much greater than anticipated by the designers. However, for the same base materials but provided lubrication via a solid gold film or via grease, the axial force does not exceed about 0.2 times the normal load even for the largest misalignment angles tested. For practical purposes, for the case of lubricated rollers the maximum attainable axial force develops for shaft angles of about 0.5 degree. These test results highlight the critical role of lubrication for the SARJ mechanism.

If the raceway of the SARJ mechanism becomes damaged, it is possible that the un-nitrided substrate will be exposed and will interact with the hardened 440C roller surface. Therefore, it was desired to study the case of un-nitrided material mating with 440C rollers in a vacuum environment. The results of these tests

with the un-nitrided material are provided in Figure 11. The data for nitrided roller is also provided on the chart for comparison. The axial force that develops for the case of un-nitrided vs. 440C with no lubrication is somewhat less than can be obtained for the nitrided surfaces. Still, with no lubrication the axial force can be high, an undesirable condition for the SARJ mechanism. Providing grease lubrication to the un-nitrided 15-5 material greatly reduces the maximum attainable axial force with the value limited to about 10 percent of the applied normal load. Comparing the data for testing with grease (Figures 10 and 11), regardless of the nitrided or un-nitrided condition the functional relationship of axial load to shaft angle is approximately the same, and the axial force is limited to about 15 percent of the normal load.

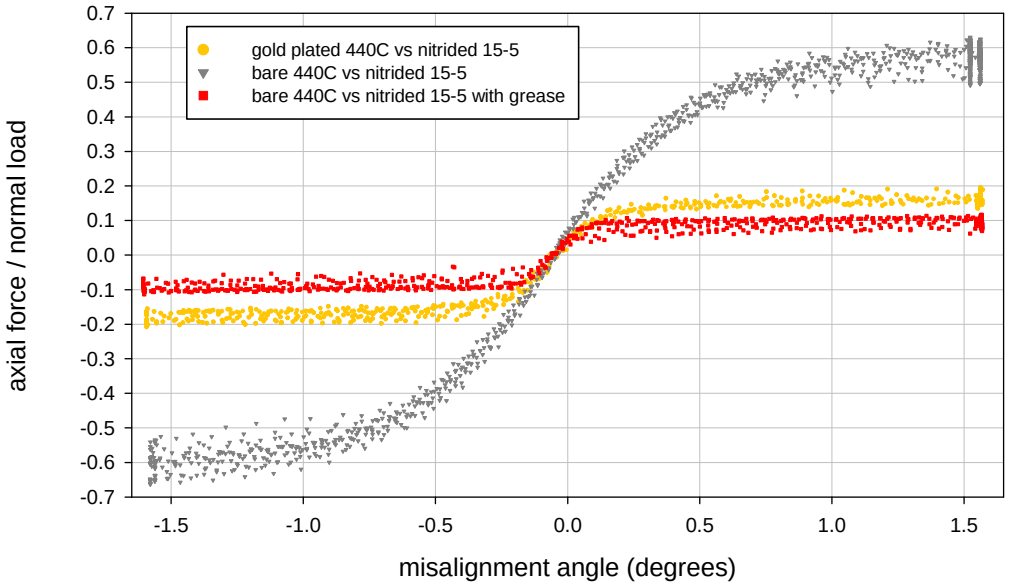

Figure 10 – Axial force as a ratio of the normal load as a function of the shaft misalignment angle when testing nitrided rollers. The data were recorded as three levels of normal load (445, 667, and 890 N) {100, 150, and 200 lb}.

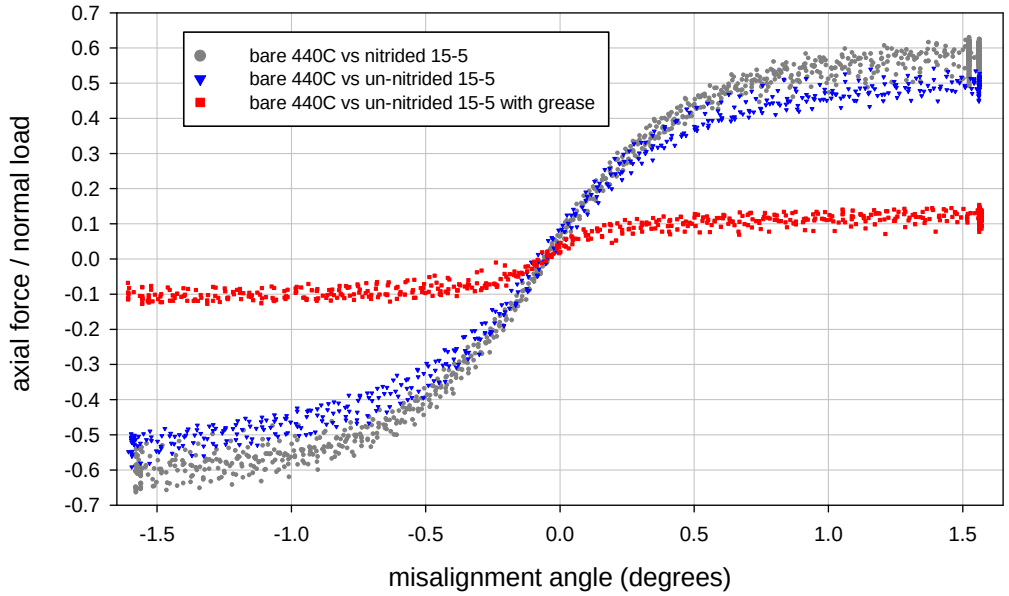

Figure 11 - Axial force as a ratio of the normal load as a function of the shaft misalignment angle when testing un-nitrided rollers. The data were recorded as three levels of normal load (445, 667, and 890 N) {100, 150, and 200 lb}. Data for nitrided rollers from Figure 10 are included for comparison.

Certain testing of the full-scale SARJ mechanism was done in an air environment. To provide some insight about the relative behavior of rollers operating in vacuum or air, a set of tests were conducted in air using a bare 440C roller and a nitrided 15-5 roller with no lubrication. The testing was done for 3 levels of normal load (445, 667, and 890 N), {100, 150, and 200 lb}. The results of the testing are provided in Figure 12. The maximum attainable axial force is slightly less when testing in air as opposed to testing in vacuum. The test was conducted using a pair of rollers that was first exposed to vacuum for testing and then exposed to air for approximately 20 minutes before starting the testing. It is recognized that this lab procedure does not necessarily recreate the surface condition of the SARJ mechanism during full-scale testing. The test data show that high magnitudes of axial force can be created when operating 440C rollers against nitrided 15-5 rollers in air.

The data of Figures 9-12 provide insight about the operation of the SARJ mechanism. Large axial forces can develop even for small magnitudes of shaft misalignment. These axial forces in the case of the SARJ mechanism act via a pivot point in the housing to produce non-uniform contact pressures across the roller width, and if the forces are of sufficient magnitude can cause roller tipping. The experiments and data demonstrate the critical role of good lubrication. The gold films provided good lubrication for the short duration testing done and reported herein. It was noted that the gold did wear away during testing, and by cursory visual inspection the gold appeared to have been removed for the contact path. However, the axial forces remained low indicating good lubrication. Close inspection of the rollers after removal from the rig with the aid of magnification revealed that the gold, while depleted in depth and coverage, was not completely worn away during these tests. The grease lubrication limited the magnitude of the axial forces that could develop to even smaller magnitudes than was achieved with the gold-film lubrication.

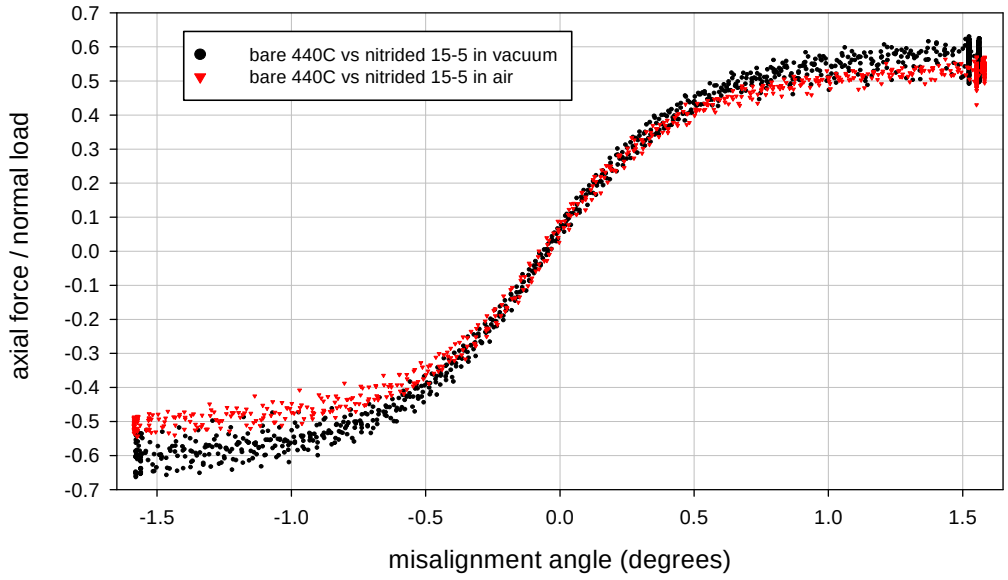

Figure 12 - Axial force as a ratio of the normal load as a function of the shaft misalignment angle when testing nitrided rollers in vacuum and in air. The data were recorded as three levels of normal load (445, 667, and 890 N) {100, 150, and 200 lb}.

Axial Force as a Function of Braking Torque with Shaft Misalignment

The data results presented in the previous section was for the condition of a small amount of torque transmitted by the rollers. To gain additional insight about the behavior of rollers in contact with shaft misalignment, a test was completed to assess the relationship of axial force as a function of the torque transmitted by the rollers for a condition of shaft misalignment of 1.5 degrees. The rollers used for this test were a bare 440C roller and a previously run nitrided 15-5 roller. The rig was operated at a speed of approximately 15 rpm. The test was done in vacuum of $5x10^{-6}$ Torr. The normal load between the rollers was 434 N (98 lb). With the test operating, the braking toque on the output shaft was steadily increased. The axial force (normalized to the normal load) as a function of the braking torque applied to the output shaft is provided in Figure 13. As the braking torque increased, the axial force decreased as should be expected and will be explained in discussion to follow. The axial force changes in a non-linear fashion with respect to the braking torque on the output shaft. The contacting region between the rollers includes both a stick and slip zones. The transition from stick to slip depends on the total traction force comprised of two orthogonal components, the axial and tangential forces. The application of additional braking torque increase the tangential component of the traction force and thereby alters the contact conditions, with the stick zones decreasing in size and the slip zones increasing in size. This test highlights that the axial force that develops when shafts are misaligned at small angles is largely the result of strains that develop in the stick region of the contact. The total traction force that can be supported by the contact is limited by the frictional condition of the mating surfaces. As was highlighted in the previous section, lubrication limits the total traction capability of the contact and thereby limits the magnitude of the axial force in response to shaft misalignment.

The trends of the data of Figure 13 demonstrate that the axial force to normal load ratio investigated herein, although having a mathematical form matching that of coefficient of friction, is not a direct measure of the coefficient of friction of the contacting surfaces. The friction condition indeed plays a primary role influencing the behavior of the contact. The axial force to normal load ratio is also influenced by the design details and by the operating conditions including the torque transferred by the roller.

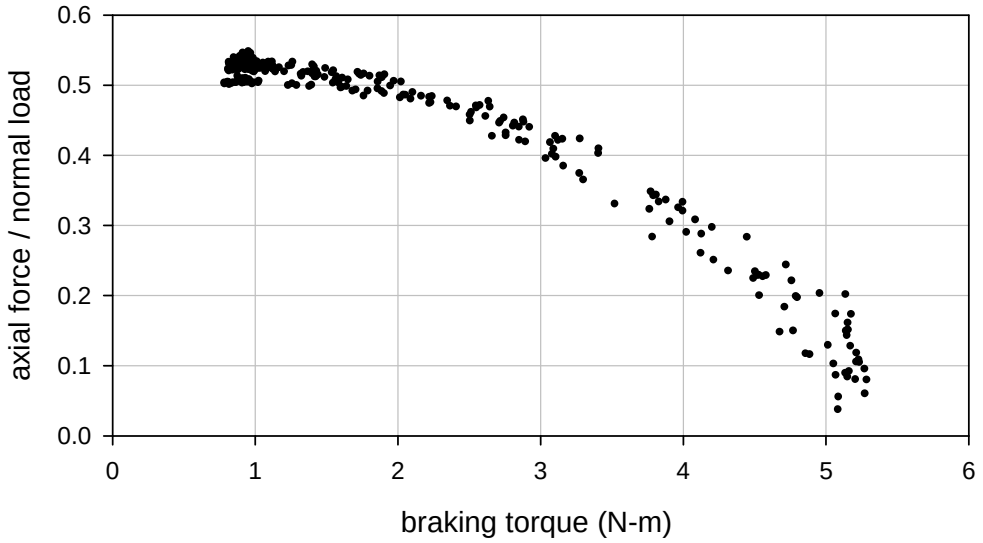

Figure 13 – Axial force as a ratio of the normal load as a function of braking torque applied to the output shaft for a bare 440C roller and a nitrided 15-5 roller operating in vacuum at 15 rpm.

Summary

A set of experiments were done using roller pairs to understand and quantify the forces that can develop for a variety of test conditions. The materials and test conditions were selected to help understand the behavior of the SARJ mechanism. Tests were done using hardened 440C rollers mated with 15-5 rollers, the 15-5 rollers being both in nitrided and bare (not nitrided) condition. Tests were done with no lubrication, solid gold-film lubrication, and grease lubrication. Of great significance to the operation of the SARJ mechanism is the magnitude of the axial force that will develop because of shaft misalignment. The experiments demonstrate the critical role of good lubrication for the SARJ mechanism. The following specific results were obtained:

1. For the case of a bare (un-plated) 440C roller against a nitrided 15-5 roller without lubrication, the axial force can be as great as 0.4 times the normal load for a shaft angle of 0.5 degree. Experiments and analysis done by others have shown that such a magnitude of force on a SARJ roller would cause roller tipping and contact pressures much greater than anticipated by the designers.

2. The axial force for the case of bare (un-plated) 440C vs. un-nitrided 15-5 with no grease is somewhat less than can be obtained using the nitrided 15-5 surfaces. Still, with no lubrication the axial force can be high, an undesirable condition for the SARJ mechanism.

3. For the case of a gold-plated 440C roller against a nitrided 15-5 roller without grease, the axial force does not exceed about 0.2 times the normal load even for the largest misalignment angles tested.

4. For the case of a bare (un-plated) 440C roller against a nitrided 15-5 roller with grease lubrication, the axial force does not exceed about 0.15 times the normal load even for the largest misalignment angles tested.

5. The experiments and data demonstrate the critical role of good lubrication. The gold films provided good lubrication for the short duration testing done and reported herein. Grease lubrication limited the magnitude of the axial force to even smaller magnitudes than was achieved with the gold-film lubrication.

6. For the case of a bare (un-plated) 440C roller against a nitrided 15-5 roller without lubrication, the maximum attainable axial force was slightly less when testing in air as opposed to testing in vacuum.

Acknowledgements

This research was supported by the NASA Engineering Safety Center. The experimental work was done with assistance from Mr. Justin Elchert of Case Western Reserve University as part of the NASA GRC LeRCIP Summer Student Program.

References

[1]. Loewenthal, S. and Schuller, F., “Feasibility study of a discrete bearing/roller drive rotary joint for the Space Station”, NASA Technical Memorandum 88800, 1986.

2. Johnson, K.L., **Contact Mechanics**, Cambridge University Press, 1985.

3. Kalker, J.J., “Rolling contact phenomena: linear elasticity”, Rolling Contact Phenomena CISM Courses and Lectures**,** Issue: 411, Springer-Verlag, 2000.

[4]. Woody, D. and Lamb, W., "A design for a precision 10-m sub-millimeter antenna", ALMA Memo 241,Mar 1999. http://www.mma.nrao.edu/memos/html-memos/alma241/memo241a.pdf, accessed Feb. 26, 2009.

[5]. McGinness, H., "Antenna azimuth bearing model experiment," DSN Progress Report 42-53, July and August 1979, Jet Propulsion Laboratory, Pasadena, Calif., 1979.

[6]. McGinness, H., "Lateral forces induced by a misaligned roller," DSN Progress Report 42-45, March and April 1978, Jet Propulsion Laboratory, Pasadena, Calif., 1978.

[7]. Hamrock, B., and Brewe, D., “Simplified Equation for Stresses and Deformations,” ASME J. Lubr. Technol., 105, pp. 171–177, 1983.